DOI: htpps://doi.org/10.3986/ac.v55i1.15079

SEASONAL CONTROL OF CAVE MICROCLIMATE BY SURFACE CONDITIONS: EVIDENCE FROM A DENSITY-DRIVEN EXCHANGE FLOW IN SAMOGRAD CAVE (CROATIA)

SEZONSKI VPLIV POVRŠINSKIH RAZMER NA MIKROKLIMO V JAMI: DOKAZI NA PODLAGI IZMENJALNEGA TOKA, KI SE SPREMINJA SKLADNO Z GOSTOTO, V JAMI SAMOGRAD (HRVAŠKA)

Nenad BUZJAK[1,2*], Franci GABROVŠEK[3], Dalibor PAAR[4], Aurel PERŞOIU[2,5], Christos PENNOS[2,6] & Valerija ROSSI[1]

Abstract

Nenad Buzjak, Franci Gabrovšek, Dalibor Paar, Aurel Perşoiu, Christos Pennos & Valerija Rossi: Seasonal control of cave microclimate by surface conditions: evidence from a density-driven exchange flow in Samograd Cave (Croatia)

This study investigates the seasonal microclimate dynamics of Samograd Cave (Croatia), a vadose karstic cave characterized by a single large entrance, a concave longitudinal profile, and active atmospheric coupling with the surface. Continuous air-temperature monitoring using data loggers was conducted along a surface-entrance-interior transect at five fixed locations over the period December 2022 – February 2024, covering two winters and one warm season. To independently assess ventilation efficiency and confirm microclimatic bimodality, air CO_2 concentrations were measured using a combination of spot monthly measurements along the cave and high-resolution continuous monitoring at the lowest point of the cave. The primary aim of the study was to evaluate how temperature differences between the surface and the cave controls seasonal air circulation and to determine whether air circulation in the cave is governed by temperature- and density-driven exchange flow. Results show that Samograd Cave exhibits a distinctly bimodal microclimate. During the cold season, negative surface-cave temperature differences promote the inflow of cold, dense air, activating an exchange flow that ventilates the cave interior and leads to an evident decrease in CO_2 concentrations. In contrast, during the warm season, such circulation is switched off, resulting in thermal stratification, microclimatic stability, and elevated CO_2 levels, with the cave acting as an efficient cold-air

Izvleček

Nenad Buzjak, Franci Gabrovšek, Dalibor Paar, Aurel Perşoiu, Christos Pennos & Valerija Rossi: Sezonski vpliv površinskih razmer na mikroklimo v jami: dokazi na podlagi izmenjalnega toka, ki se spreminja skladno z gostoto, v jami Samograd (Hrvaška)

Ta študija proučuje sezonsko spreminjanje mikroklime v jami Samograd (Hrvaška), ki je vadozna kraška jama s samo enim velikim vhodom, konkavnim vzdolžnim profilom in aktivnim atmosferskim medsebojnim delovanjem s površino. Od decembra 2022 do februarja 2024, tj. v dveh zimah in enem toplem letnem času, je potekalo neprekinjeno spremljanje temperature zraka s podatkovnimi zapisovalniki vzdolž profila, ki je zajemal površino, vhod in notranjost, na petih fiksnih lokacijah. Za neodvisno oceno učinkovitosti prezračevanja in potrditev mikroklimatske bimodalnosti so bile koncentracije CO_2 v zraku izmerjene s kombinacijo mesečnih točkovnih meritev vzdolž jame in neprekinjenega spremljanja z visoko časovno ločljivostjo na najnižji točki jame. Glavni cilj študije je bil ugotoviti, kako temperaturne razlike med površino in jamo vplivajo na sezonsko kroženje zraka ter ali na kroženje zraka v jami vpliva izmenjevalni tok, ki se spreminja skladno s temperaturo in gostoto. Iz rezultatov je razvidno, da v jami Samograd prevladuje izrazita bimodalna mikroklima. V hladnem letnem času negativne temperaturne razlike med površino in notranjostjo jame spodbujajo dotok hladnega, gostega zraka, zaradi česar nastane izmenjevalni tok, ki prezračuje notranjost jame, ob tem se opazno zmanjšajo koncentracije CO_2. Nasprotno pa se v toplem letnem času takšno kroženje zraka ustavi, posledica česar so toplotni sloji, mikroklimatska stabilnost in zvišane ravni CO_2, jama pa deluje kot učinkovit zadrževalnik

[1] University of Zagreb Faculty of Science, Department of Geography, Croatia, e-mail: nenad.buzjak@geog.pmf.unizg.hr
[2] Emil Racoviță Institute of Speleology, Romanian Academy, Cluj-Napoca, Romania
[3] Karst Research Institute ZRC SAZU, Postojna, Slovenia, e-mail: franci.gabrovsek@zrc-sazu.si
[4] University of Zagreb Faculty of Science, Department of Physics, Croatia, e-mail: dpaar@phy.hr
[5] Stable Isotope Laboratory, Ștefan cel Mare University, Suceava, Romania, e-mail: aurel.persoiu@acad-cj.ro
[6] School of Geology, Department of Physical Geography, Aristotle University of Thessaloniki, Greece, e-mail: cpennos@auth.gr
[*] Corresponding author

Received/Prejeto: 7. 2. 2026

trap. Statistical analysis of air-temperature variability, surface-cave correlations, and CO_2-temperature relationships demonstrates that the magnitude and persistence of seasonal thermal gradients, rather than the frequency of cold events alone, govern ventilation intensity. The combined temperature and CO_2 evidence provides robust confirmation of the seasonal coupling between surface conditions and cave microclimate and supports the interpretation of Samograd Cave as a bimodal microclimate system.
Keywords: cave microclimate, bimodality, winter ventilation, density-driven circulation, Dinaric karst.

hladnega zraka. Statistična analiza spremenljivosti temperature zraka, korelacij med površino in jamo ter odnosov med CO_2 in temperaturo kaže, da intenzivnost prezračevanja uravnavata predvsem obseg in trajanje sezonskih temperaturnih gradientov, ne le pogostost nizkih temperatur. Kombinirani podatki o temperaturi in ravneh CO_2 zagotavljajo trdno potrditev vpliva letnih časov na razmere na površju in mikroklimo v jami ter podpirajo razlago, da je jama Samograd bimodalni mikroklimatski sistem.
Ključne besede: mikroklima v jami, bimodalnost, zimsko prezračevanje, kroženje zraka, na katero vpliva gostota, Dinarski kras.

1. INTRODUCTION

In caves developed within the vadose zone, where atmospheric connectivity is preserved, air circulation (besides occasional infiltrating precipitation) constitutes a major and all-time present mechanism of fast energy transfer that can induce substantial thermal variability at different spatial and temporal scales (Perşoiu et al., 2021). In such settings, the penetration of external climatic signals into the underground is neither uniform nor permanent, but depends on surface topography, cave morphology, length and depth, entrance configuration, and the efficiency of heat exchange along air and water pathways.

Early microclimatic observations demonstrated that caves are characterized by spatially differentiated thermal regimes. Based on long-term air temperature measurements in caves of the Polish Tatra Mountains, Pulina (1968) distinguished a dynamic entrance zone, where air temperature exhibits pronounced daily and seasonal oscillations linked to external conditions, and a deeper comparatively static inner zone in which temperature variability is strongly attenuated. Importantly, this zonation was defined empirically through the amplitude of air temperature fluctuations rather than through assumptions of thermal equilibrium, implying that "static" conditions correspond to damped variability rather than to constancy. A complementary, process-based perspective was later provided by studies of the thermal field in karst massifs. Drogue (1985) introduced the distinction between heterothermic zones, where external or internally induced thermal perturbations propagate into the underground, and homothermic zones, where the thermal regime is comparatively stable. In this framework, the depth and spatial extent of the heterothermic zone are controlled not by depth alone but by the structure and permeability of the karst system, as well as by the dominant modes of heat transfer. This concept was further quantified by Luetscher and Jeannin (2004), who showed that in the vadose zone the thermal regime is largely governed by advective heat transport associated with air circulation, whereas conductive heat transfer and geothermal flux dominate at greater depth and in phreatic conditions. Their results demonstrate that homothermic conditions in vadose caves are characterized by low seasonal amplitudes and persistent vertical temperature gradients rather than by uniform temperatures. The interpretation of cave temperature as a simple proxy for mean annual surface air temperature has therefore been shown to be an oversimplification. Badino (2010) explicitly decomposed this approximation by demonstrating that deeper in the cave, air temperature may only approach the temperature of the surrounding rock mass, which itself is strongly influenced by infiltrating meteoric water during long periods of time. Its temperature can systematically deviate from local mean air temperature due to altitude effects, seasonal concentration of precipitation, and selective infiltration processes. Moreover, airflow-driven convection introduces additional spatial and seasonal disequilibria, particularly in caves with active ventilation. As a result, thermally "stable" cave environments should be understood as systems with attenuated variability rather than as thermally invariant systems. Recent studies have further emphasized the seasonal nature of cave ventilation and its role in shaping cave microclimate. Studies of vertically developed vadose caves have shown that airflow regimes are commonly organized into alternating winter and summer modes, driven primarily by the temperature difference between the external and cave atmosphere (ΔT). During periods of large negative ΔT, cold dense air penetrates the cave and promotes circulation. During warm periods, thermal stratification suppresses air exchange and leads to temporary decoupling from short-term surface variability (Gil et al., 2025). These findings demonstrate that stable temperature regimes can emerge as transient states associated with sustained airflow, rather than as expressions of long-term thermal equilibrium.

Within this conceptual framework, cave microclimate can be interpreted as the outcome of seasonally activated processes that govern the penetration depth and the temporal persistence of external thermal signals. The spatial reach of these signals is constrained by cave geometry and ventilation efficiency, while their temporal expression is controlled by the magnitude and duration of surface-underground temperature differences. Continuous, spatially distributed temperature measurements are therefore essential for identifying the conditions under which temperature-driven circulation develops and for distinguishing between dynamically ventilated and thermally damped cave sectors.

This study builds on this theoretical background by analyzing microclimate measurements from Samograd Cave (Croatia). By combining surface, entrance, and interior air temperature records, the study focuses on the seasonal coupling between external conditions and cave microclimate, with particular emphasis on the winter period characterized by increasing ΔT between external atmosphere and cave. Through statistical analysis of air temperature dynamics and their spatial coherence, the cave is interpreted as a seasonally activated, temperature-driven ventilation system, while CO_2 concentrations are used as an independent indicator of ventilation. This approach provides a process-oriented assessment of surface-driven cave microclimate dynamics grounded in established theoretical concepts and supported by high-resolution empirical data.

2. STUDY SITE

Samograd Cave is located in the Lika region of Croatia, within the karst area of the Grabovača Cave Park near Perušić (Buzjak et al., 2020; Figure 1). The cave is situated in a temperate continental climate (Köppen–Geiger type Cfb; Filipčić, 1998), characterized by pronounced seasonal temperature contrasts. Due to the predominance of karst landforms, particularly the high proportion of large karst depressions (poljes, uvalas, and large dolines), local climatic conditions are occasionally modified by temperature inversions. This climatic setting provides favorable conditions for seasonally variable surface-underground thermal gradients, which are essential for the development of temperature-driven air circulation in caves.

The cave has a single entrance (6 m wide and up to 4 m high), oriented towards the north and located at an elevation of 678 m a.s.l., opening at the bottom of a large collapsed doline. From the entrance, the cave continues into a longitudinally developed passage with a distinctly concave profile morphology (Figure 1). The passage initially descends toward a lower interior section and then gradually rises toward the cave end. Such a geometry promotes the accumulation of cold, dense air in deeper sections during periods of winter cooling, while favoring thermal stratification and reduced air exchange during warm-season conditions (Buzjak et al., 2024). The overall morphology therefore provides a suitable natural configuration for investigating seasonally activated airflow driven by air temperature and associated density contrasts, and its spatial extent within the cave. The total mapped length of the cave is 346 m, and the lowest point is situated 53 m below the surface. Samograd Cave is developed entirely within the vadose zone, with no permanent water bodies present in the monitored sections. Infiltrating meteoric water is present, but its thermal influence is indirect and mediated through interactions with the surrounding rock mass. The cave has been adapted for tourism; however, visitor numbers are relatively low, resulting in limited anthropogenic disturbance of the cave atmosphere. A previous work (Buzjak et al., 2024) showed that natural ventilation processes dominate the seasonal behavior of cave air temperature and gas concentrations, while short-term anthropogenic effects remain subordinate. This makes Samograd Cave a suitable site for analyzing natural microclimatic dynamics of a vadose cave.

3. METHODS AND DATA ANALYSIS

Microclimate monitoring was conducted using temperature and relative humidity data loggers Onset HOBO U23 Pro v2 (temperature sensor accuracy ±0.2°C from 0 to 70°C, resolution 0.04°C; ONSET Hobo, USA) installed at five fixed locations (SG-1 to SG-5; Figure 1), forming a longitudinal surface-cave entrance-cave interior transect.

Measurements covered the period 1 December 2022– 29 February 2024, with a sampling interval of 1 h. This period spans a complete annual cycle of climatically defined seasons, including two winters and intervening spring, summer and autumn months, enabling robust characterization of seasonal microclimatic variability, improved interpretation of temperature-driven ventilation processes and surface-cave interior coupling. All loggers installed inside the cave were mounted in plastic holders attached to 5-mm-thick plastic plates to provide thermal isolation from the rock. The assemblies were fixed to the cave wall at approximately 0.5 m above the cave floor in order to minimize direct conductive influence from the ground and to ensure comparability of air temperature measurements across sites.

Logger SG-1 was installed inside a naturally ventilated white plastic solar radiation shield (Stevenson-type, model Onset RS1) mounted on a tree at a height of 2 m above ground level on the forested slope north of the Samograd collapsed doline rim and collecting data about external atmospheric conditions. The position of SG-1 was determined using the Locus Map application, with a reported positional accuracy of approximately 2 m (coordinates: N 44.64307, E 15.355305), at an elevation of 693 m a.s.l. Logger SG-2 was positioned in front of the cave entrance, at the bottom of a collapsed doline, where surface and subterranean influences overlap. Logger SG-3 was the first one installed in the cave - in the entrance chamber, at a distance of 45 m from the cave entrance line and 17.5 m below the entrance, representing the proximal cave interior. Logger SG-4 was positioned at the lowest point of the cave, 133 m from the entrance and 40.3 m below the entrance level, corresponding to a depth of 52.7 m below the entrance level. Logger SG-5 was installed at the highest interior point of the cave, 204 m from the entrance and 12.4 m above the cave entrance level, representing the upper interior section of the cave.

Carbon dioxide (CO_2) concentrations were monitored using two complementary approaches that differ in temporal resolution and analytical purpose. Monthly CO_2 measurements were performed at all monitoring locations (SG-1 to SG-5) using a portable CO_2 meter AZ77535 (CO_2 sensor accuracy 0~5000 ppm: ±30 ppm ±5% of reading, resolution 1 ppm; AZ Instrument Corp., Taiwan). Measurements were conducted typically around the middle of

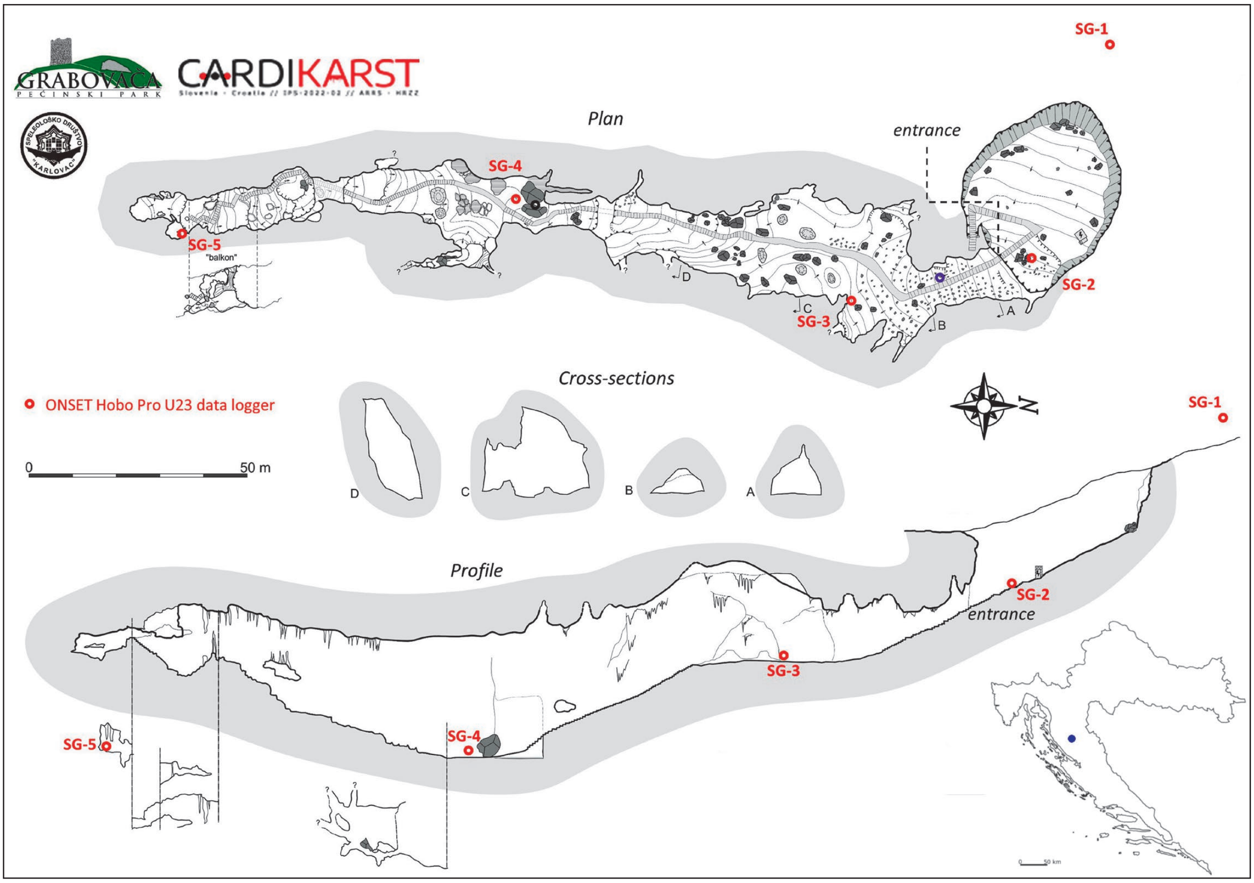

Figure 1. Samograd cave geographical position and cave map with loggers' locations. Map by Neven Bočić & Dinko Stopić (Caving Club Karlovac), 2011.

each month, and represent instantaneous point observations of CO_2 concentration at the time of measurement. These data were used to characterize seasonal and spatial patterns of CO_2 distribution within the cave and to assess its relationship with temperature-derived ventilation proxies at a monthly timescale. Hourly CO_2 measurements were carried out at the interior site SG-4 (ground level; Figure 1), as the deepest point, using a CO_2 data logger CM-0018 (CO_2 sensor accuracy ±30ppm, ±3% measured value, resolution 1 ppm; CO2Meter, USA). The logger recorded CO_2 concentration at an hourly interval for most of the study period. Two data gaps occurred due to temporary logger battery malfunction, from 16 July to 18 August 2023 and from 17 September to 22 October 2023. Together, these two CO_2 datasets allow assessment of both the long-term, integrated response of cave air composition to seasonal ventilation forcing and the short-term temporal behavior of CO_2 during periods of sustained or transient thermal gradients.

Although air temperature, relative humidity, and dew point were recorded at all monitoring sites, air temperature was selected as the primary analytical variable because the focus of this study is seasonal density-driven air circulation and its coupling with external atmospheric conditions. In caves, the forces responsible for airflow arise from temperature-controlled density contrasts between external and cave air masses; therefore, the surface-cave temperature difference (ΔT) provides the most direct physical link between external forcing and internal airflow response (Badino, 2010; Luetscher & Jeannin, 2004). Cave air temperature represents an emergent system-level variable produced by the interaction of convective airflow, heat exchange with the surrounding rock mass, and time-dependent external boundary conditions (Badino, 2018). Empirical studies have shown that in vadose caves advective heat transport may dominate over conductive and moisture-related effects, and that temperature fields can serve as diagnostic indicators of airflow intensity and direction (Luetscher & Jeannin, 2004; Gil et al., 2025). In contrast, relative humidity in humid cave environments often remains near saturation and primarily reflects thermodynamic adjustment processes rather than airflow regime switching (De Freitas, 1987). Similar systems have demonstrated that temperature variations are, by and large, the dominant driver of density-driven ventilation (Gabrovšek, 2023). Taken together, these considerations justify the use of air temperature and ΔT as the core analytical basis.

4. RESULTS

4.1. AIR TEMPERATURE CHARACTERISTICS FOR THE ENTIRE MONITORING PERIOD

Minimum and maximum air temperatures show a pronounced spatial gradient along the surface-entrance-interior transect (Table 1). At the surface (SG-1), air temperature ranged from -9.95 °C to 34.02 °C, while at the entrance zone (SG-2) it ranged from -8.10 °C to 24.53 °C, indicating strong exposure to external atmospheric forc-

Table 1. Descriptive statistics of air temperature (°C) at locations SG-1 to SG-5 for the entire observation period (December 2022 – February 2024).*

Statistical Parameter	SG-1	SG-2	SG-3	SG-4	SG-5
Minimum (°C)	−9.95	−8.10	−1.33	1.48	7.62
Maximum (°C)	34.02	24.53	7.17	6.51	8.57
Range (°C)	43.97	32.63	8.49	5.03	0.95
Mean (°C)	9.62	7.65	5.12	5.08	7.88
Median (°C)	9.09	6.95	5.39	5.23	7.87
Mode (°C)	8.17	6.00	7.07	6.26	7.87
Standard Error (°C)	0.076	0.059	0.015	0.009	0.001
Standard Deviation (°C)	7.99	6.15	1.59	0.94	0.13
Sample Variance	63.86	37.78	2.52	0.88	0.02
Skewness	0.22	0.00	−0.83	−0.71	−0.36
Kurtosis	−0.45	−0.98	0.20	−0.02	−0.79

**The descriptive statistics are calculated for the entire monitoring period and therefore integrate two cold seasons and one warm season; the resulting distribution parameters reflect the seasonal asymmetry of the dataset rather than equal seasonal weighting.*

ing. In the part of the passage under direct external influence (SG-3), minimum temperatures reached -1.33 °C, confirming penetration of cold air into the cave during winter episodes, evidenced by frozen dripwater and ice stalagmites near the entrance zone. At the lowest point of the cave (SG-4), minimum temperature remained positive (1.48 °C), indicating substantial attenuation of extreme surface cooling. At the upper site (SG-5), air temperature was confined to a narrow interval between 7.62 °C and 8.57 °C, indicating almost no direct influence of cold air intrusion. The temperature range decreases systematically, from 32.63 °C at SG-2 to 8.49 °C at SG-3 and 5.03 °C at SG-4, reaching only 0.95 °C at SG-5. This pattern corresponds to the progressive damping of temperature variability (Figure 2).

Mean air temperature decreases from SG-1 (9.62 °C) toward the lower interior sites SG-3 (5.12 °C) and SG-4 (5.08 °C), indicating comparable long-term thermal conditions in these parts of the cave. In contrast, the upper interior site SG-5 exhibits a higher mean temperature (7.88 °C), reflecting a distinct thermal regime. Median values closely follow mean values at all locations, indicating that temperature distributions are not dominated by isolated extreme events. Mode values further differentiate surface and interior thermal regimes. At SG-1 and SG-2, modal temperatures correspond to frequently occurring atmospheric conditions, whereas at SG-3 and SG-4 modal values cluster within a narrow interval, reflecting stable interior temperatures intermittently affected by winter cooling. At SG-5, the coincidence of mean, median, and mode values, together with the very small temperature range and low dispersion, indicates a thermally buffered zone primarily controlled by heat exchange with the surrounding rock mass. Positioned higher in the cave and outside the main pathway of winter cold-air inflow, this section remains largely decoupled from temperature-driven circulation. This behavior is consistent with the vertical temperature stratification (Figure 2), where colder air occupies the lower cave sections during winter, while the upper interior remains thermally stabilized by conductive heat exchange with the cave walls.

Dispersion measures show a strong spatial differentiation. Standard deviation decreases from 7.99 °C at SG-1 and 6.15 °C at SG-2 to 1.59 °C at SG-3 and 0.94 °C at SG-4, reaching only 0.13 °C at SG-5. Corresponding variance values follow the same pattern, confirming progressive attenuation of temperature fluctuations toward the cave interior. Standard error values also decrease sys-

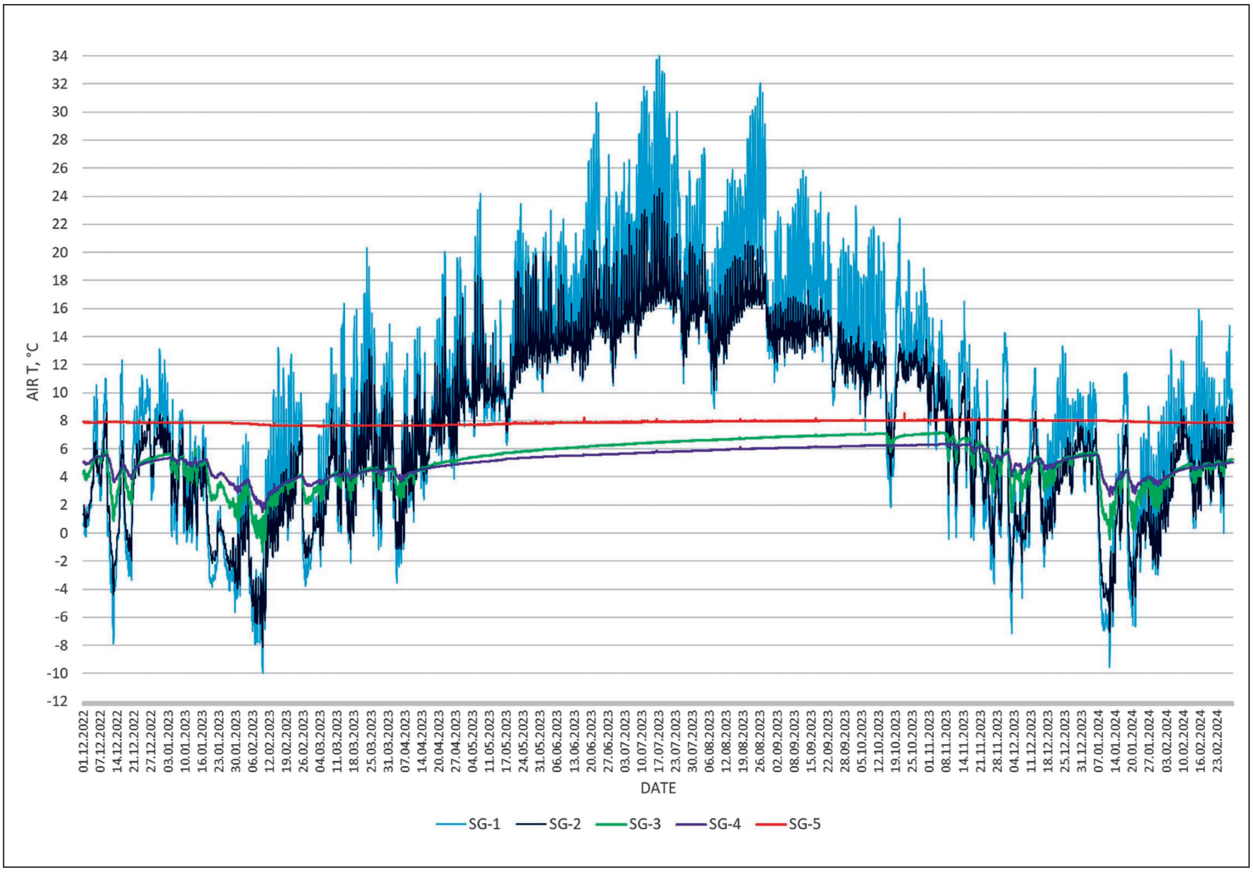

Figure 2. Air temperature time series at all locations SG-1 to SG-5 for the entire observation period (December 2022 – February 2024).

tematically from the surface toward the interior, indicating increasing temporal stability of mean air temperature deeper in the cave.

Distribution shape parameters further distinguish thermal regimes. Near-zero positive skewness at SG-1 and 0.00 at SG-2 indicates relatively symmetric temperature distributions associated with alternating cold and warm periods. Negative skewness at SG-3 and SG-4 reflects temperatures intermittently affected by winter cooling events. Slight negative skewness at SG-5 is consistent with a narrowly constrained distribution. Kurtosis values close to zero at SG-3 and SG-4 indicate near-normal distributions, whereas negative kurtosis reflects either strong variability (SG-1 and SG-2) or pronounced stability (SG-5).

4.2. MONTHLY DYNAMICS

Monthly air temperature dynamics provide a detailed view of the temporal dynamics of surface-cave coupling and allow identification of periods of enhanced ventilation and thermal stability. Monthly mean air temperatures (Figure 3) show that external SG-1 exhibits the largest annual amplitude. At SG-2, the same seasonal pattern is preserved but with a clearly reduced amplitude, reflecting partial buffering within the collapse doline. Monthly means at SG-3 and SG-4 decrease markedly during winter months, reaching values close to 3-4 °C, whereas during the warm season they remain confined to a narrow interval around 6-7 °C. These lower sections are directly affected by episodic winter inflow of cold, dense surface air, while ventilation is suppressed during the warm season. In contrast, SG-5 displays a distinct behavior, with monthly mean temperatures remaining nearly constant throughout the year (approximately 7.8–8.0 °C). Notably, the annual minimum at this location occurs with a delay of approximately one month relative to the lower cave sites, indicating the absence of direct advective cooling and reflecting the dominant conductive thermal influence of the surrounding rock mass.

Mean surface air temperature at SG-1 (9.62 °C) provides a fixed thermal reference against which monthly cave temperatures can be evaluated. At SG-1 itself, monthly mean temperatures oscillate widely around this value, reflecting direct atmospheric forcing and high temporal variability. In contrast, all cave locations (from SG-2 to SG-5) remain persistently below the SG-1 mean

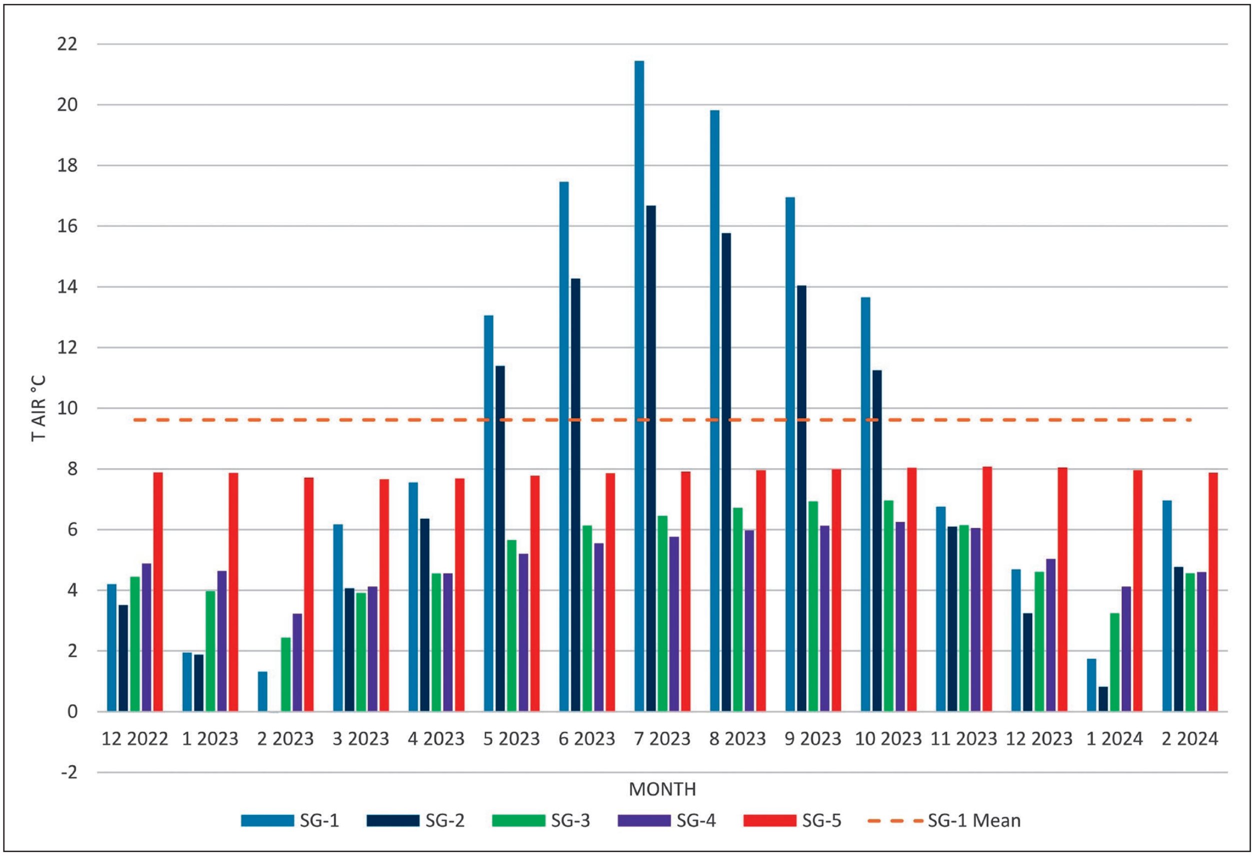

Figure 3. Monthly mean air temperatures at monitoring locations SG-1 to SG-5, with the long-term mean SG-1 indicated as a reference (December 2022 – February 2024). Note: The mean temperature at SG-2 in February 2023 was -0.02 °C; due to the y-axis scale, this value is not visually distinguishable from 0 °C in the figure.

throughout the entire observation period. This offset demonstrates that the cave system does not thermally equilibrate with mean surface conditions, but instead acts as a cold-air reservoir whose thermal state is controlled by seasonal ventilation and internal heat exchange rather than by average atmospheric temperature. The difference between the mean surface air temperature at SG-1 calculated for the entire monitoring period (9.62 °C) and the monthly mean temperatures at SG-3 and SG-4 is smallest during summer, when external temperatures are high but cave ventilation is suppressed, and largest during winter, when external temperatures drop sharply and cold-air inflow propagates into the cave. This seasonal asymmetry confirms that thermal coupling between the surface and the cave is active only during the cold part of the year, and that the magnitude of this coupling is governed by the sign and strength of the surface-cave temperature gradient. SG-5 monthly mean temperatures remain tightly clustered around 7.8-8.0 °C and show no tendency to converge toward the SG-1 mean, even during prolonged warm periods. This indicates that this zone is effectively decoupled from surface temperature fluctuations and remains mostly controlled by conductive heat exchange with the surrounding rock mass. The persistent separation between SG-5 monthly means and the SG-1 reference further highlights the vertical thermal stratification within the cave and identifies SG-5 as a stable thermal reference for the interior system. Overall, the position of monthly cave temperatures relative to the SG-1 mean demonstrates that mean surface temperature is not a predictor of cave air temperature, and that seasonal deviations from this mean constitute the primary driver of air exchange and internal thermal zonation.

Monthly standard deviation (SD) values (Figure 4A) quantify the temporal variability at each location and clearly differentiate ventilation-sensitive (SG-3 & SG-4) and more stable cave zones (SG-5). At SG-1, monthly SD remains high throughout the year, reflecting strong atmospheric variability. At SG-2, SD values are lower due to the location inside collapsed doline, but still exhibit pronounced winter maxima, indicating persistent but attenuated transmission of external temperature fluctuations. Within the cave and oriented directly towards entrance, SG-3 shows a distinct seasonal contrast: monthly SD increases from summer values below approximately 0.3 °C to winter values exceeding 1 °C, with maxima during January and February, indicating episodic cold-air incursions. At SG-4, SD values are lower than at SG-3 but still show a clear winter signal, with monthly SD increasing from <0.2 °C during the warm season to approximately 0.4-0.5 °C during winter months, confirming intermittent activation of ventilation at the lowest part of the cave. In contrast, SG-5 exhibits extremely low SD values throughout the year, frequently <0.05 °C, demonstrating exceptional thermal stability and effective isolation from short-term atmospheric variability.

Monthly skewness values (Figure 4B) clearly differentiate ventilation-affected and thermally stable parts of the cave. At SG-3 and SG-4, skewness becomes persistently negative during the cold season, with values commonly reaching approximately -0.5 and locally approaching -0.7 to -0.8 in mid-winter months. This indicates distributions dominated by winter short-lived cooling events. During the warm season, skewness at both locations shifts toward values close to zero, consistent with near-symmetric temperature distributions under weakly ventilated and stratified conditions. At SG-5, occasional months show numerically high skewness values. Inspection of the hourly record indicates that these values are driven by one or two short-lived temperature spikes, which can strongly affect skewness under the extremely low-variability regime at this site and may reflect transient local disturbances (e.g., observer presence during manual measurements or sporadic visitors), rather than airflow-related asymmetry. Since these spikes represent physically recorded but transient perturbations rather than measurement errors, the raw dataset was retained, and skewness at SG-5 is interpreted cautiously. The disproportionate influence of such brief events further illustrates the exceptional thermal stability of this sector, where even minimal perturbations produce amplified statistical responses without indicating systematic ventilation dynamics.

Monthly kurtosis values (Figure 4C) further highlight differences in the temporal structure of temperature variability within the cave. At SG-3 and SG-4, kurtosis increases during winter months, typically reaching values on the order of 1-3, indicating the presence of infrequent but distinct cooling events superimposed on an otherwise stable thermal background. During the warm season, kurtosis values generally decrease and remain low, indicating a more evenly distributed and homogeneous temperature variability under weakly ventilated and stratified conditions. At SG-5, monthly kurtosis reaches very high positive values, particularly during the warm season, frequently exceeding 10 and temporarily surpassing 100. These extreme values do not indicate intense thermal events, but instead arise from the statistical effect of an exceptionally narrow temperature range, in which rare and very small deviations from the mean are emphasized relative to the overall variability. Inspection of the hourly record shows that such elevated kurtosis values are driven by one or two short-lived temperature spikes within otherwise highly stable monthly series. Because temperature variability at this site is extremely low (monthly ranges typically 0.1-0.6 °C), even minimal per-

Figure 4. A – Monthly SD values SG-1 - SG-5. B – Monthly skewness values SG-1 - SG-5. C – Monthly kurtosis values SG-1 - SG-4 (left vertical axis) and SG-5 (right vertical axis)

turbations can disproportionately influence higher-order distributional parameters. Two of the identified spikes coincide with confirmed observer presence during manual measurements, while others likely reflect transient local disturbances rather than systematic airflow processes. The observed monthly ranges substantially exceed the instrumental resolution of 0.04 °C of the U23 logger, indicating that the recorded variability reflects physical thermal behavior rather than quantization effects. This behavior is consistent with a strongly buffered thermal regime controlled primarily by conductive heat exchange with the surrounding rock mass.

4.3. SEASONAL DYNAMICS

Seasonal air-temperature dynamics in Samograd Cave are governed by the contrast between the winter and summer conditions, reflecting seasonal changes in surface-cave thermal gradients and the activation or suppression of ventilation. Seasonal mean temperatures (Figure 5A) show that winter conditions propagate into the lower parts of the cave, whereas the warm season is characterized by thermal stabilization and stratification within the interior. During winter (December-February), mean air temperatures at SG-1 decrease to approximately 2.5-4.4 °C, creating a pronounced negative temperature difference relative to the cave interior. This gradient is reflected by a clear cooling response at SG-3 and SG-4, where winter mean temperatures decrease to about 3.7-4.6 °C and 4.3-4.6 °C, respectively. At the same time, temperature variability increases markedly: SD during winter reaches 1.48 °C and 1.28 °C at SG-3 and 0.94 °C and 0.69 °C at SG-4 during the two monitored winters (Figure 5B). Seasonal skewness remains negative at both locations (e.g., -0.62 to −0.98), indicating distributions dominated by episodic cooling events. Kurtosis exhibits pronounced interannual variability. Winter 2022/2023 shows markedly elevated kurtosis values at SG-3 and SG-4 relative to the warm season. In contrast, Winter 2023/2024 displays substantially lower kurtosis values at these locations, indicating weaker or less frequent ventilation pulses. At SG-5, high kurtosis during the Winter 2022/2023 results from the statistical sensitivity of an exceptionally narrow temperature range to short-lived perturbations, whereas Winter 2023/2024 exhibits negative kurtosis values, indicating a flatter distribution without pronounced extremes. This pattern highlights significant interannual variability in winter ventilation intensity and thermal response within the cave. In contrast,

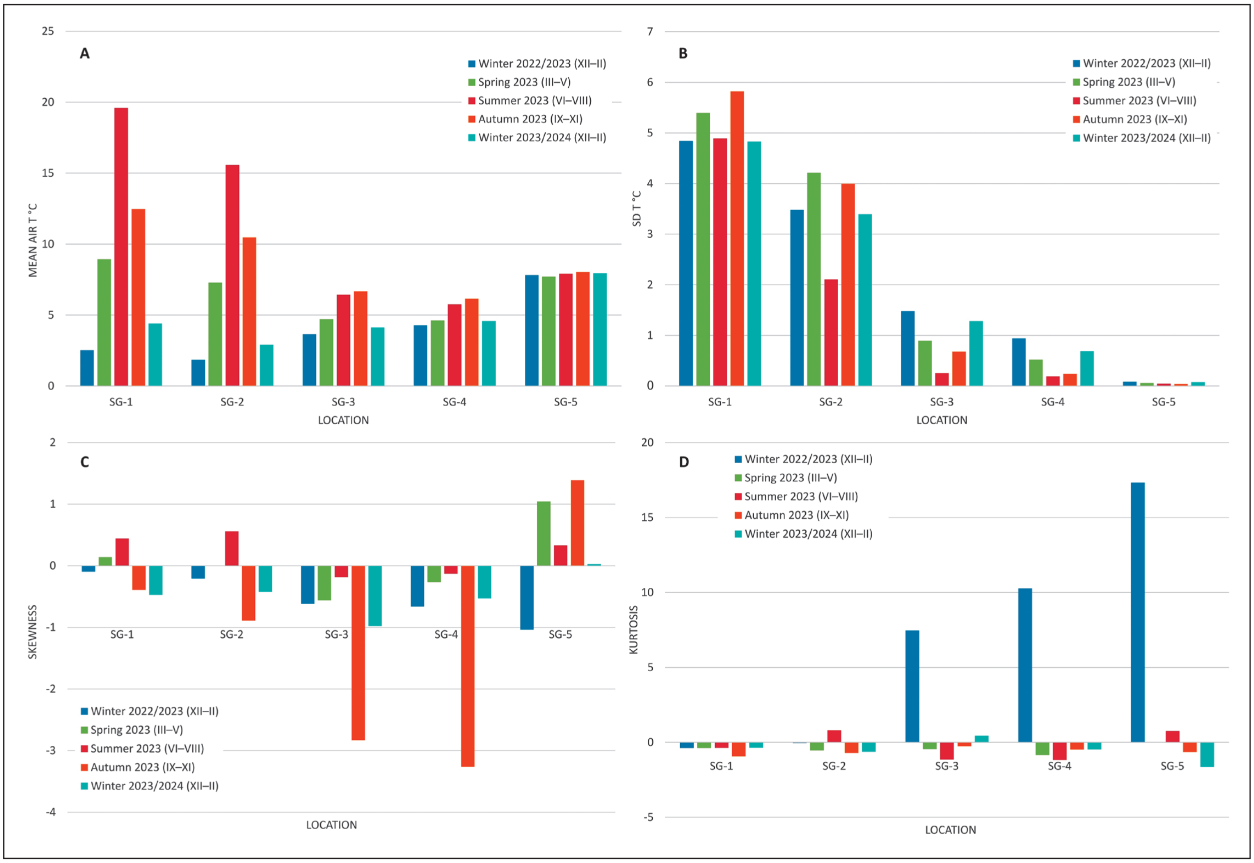

Figure 5. A – Seasonal mean air T. B – Seasonal air T SD. C – Seasonal air T skewness. D – Seasonal air T kurtosis.

SG-5 maintains significantly higher winter mean temperatures, remaining close to 7.8–8.0 °C, and shows only minimal seasonal variability. Winter SD values remain below 0.1 °C, skewness approaches symmetry (e.g., 0.02 in Winter 2023/2024), and kurtosis values at SG-5, when elevated, reflect the statistical effect of extremely narrow temperature range rather than intense thermal events (Figure 5D). During summer (June-August), surface temperatures increase substantially, with seasonal mean temperatures at SG-1 exceeding 19 °C, but this warming is not transmitted into the cave interior. Mean temperatures at SG-3 and SG-4 remain constrained to a narrow interval of approximately 5.6-6.7 °C, while SD decreases sharply to 0.25 °C at SG-3 and 0.19 °C at SG-4. Skewness values approach zero and kurtosis becomes negative at both locations, indicating symmetric and uniformly distributed temperatures under conditions of suppressed ventilation and stable stratification. SG-5 remains effectively unchanged, with seasonal means close to 8 °C and persistently minimal variability.

The monthly and seasonal evolution of mean temperature, variability, skewness, and kurtosis demonstrates that Samograd Cave operates under two distinct thermal regimes: a winter ventilation regime characterized by enhanced variability and event-dominated distributions in the lower interior (SG-3 and SG-4), and a summer regime marked by strong thermal stability, cold-air trap effect and stratification throughout the cave. Transitional seasons further refine this pattern. In autumn, several interior locations record the highest seasonal mean temperatures, reflecting the thermal inertia accumulated during preceding warm period. At the same time, skewness values at SG-3 and SG-4 indicate the onset of intermittent cooling pulses preceding full winter ventilation. The persistent stability of SG-5 across all seasons confirms its role as a thermally buffered upper cave reference and shows constraints of the vertical and longitudinal extent of seasonally active ventilation.

4.4. CORRELATION AND REGRESSION ANALYSIS

The correlation and regression analysis quantify the degree to which surface air temperature (SG-1) controls thermal conditions along the surface-cave entrance-cave interior transect and reveals a clear spatial attenuation of this impact within the cave (Figure 6). Scatter plots based on hourly data for the entire observation period show a systematic weakening of the statistical relationship between SG-1 and successive cave locations, reflecting both geometric constraints and seasonal ventilation dynamics. The strongest and most linear relationship is observed between SG-1 and SG-2, with a very high correlation coefficient (r ≈ 0.96) and a coefficient of determination exceeding 0.9. The narrow, elongated point cloud and the near-linear regression confirm that the entrance zone closely follows surface temperature variations, albeit with reduced amplitude due to the topographic position in collapsed doline. At SG-3, the relationship with surface temperature remains strong but becomes distinctly non-linear (r ≈ 0.80). The scatter plot shows a clear curvature and saturation effect at higher surface temperatures, in-

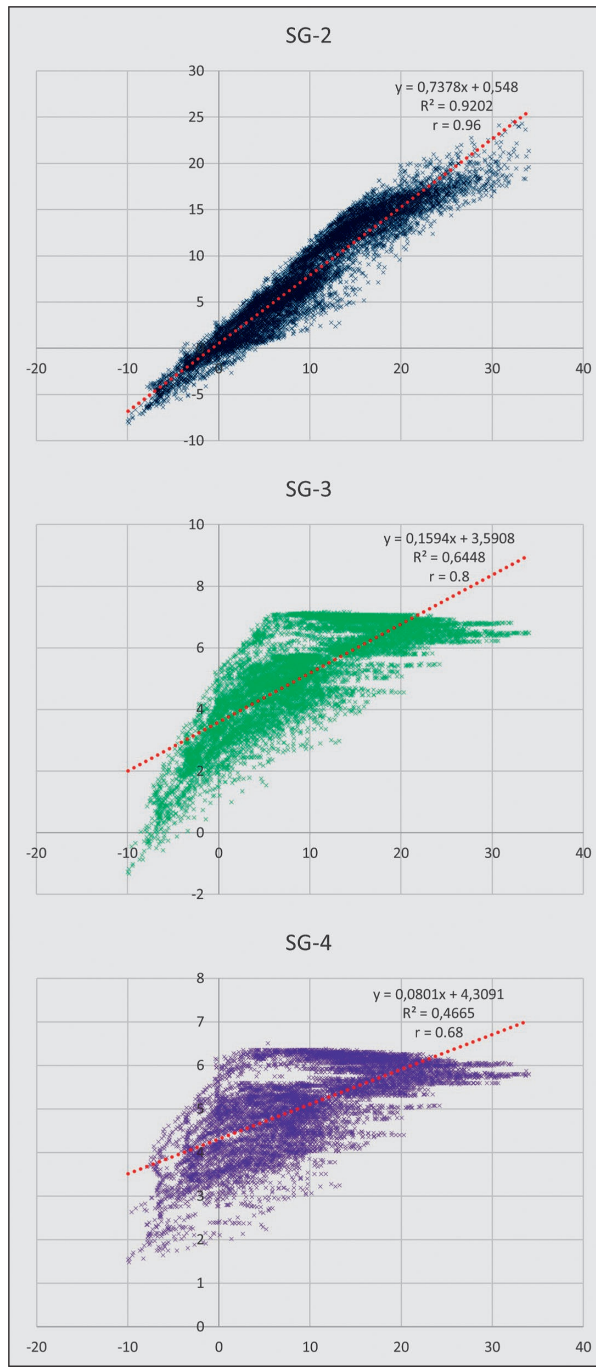

Figure 6. Scatter plots and linear regression relationships between surface air temperature (SG-1) and cave air temperature at locations SG-2, SG-3, and SG-4 for the entire observation period.

dicating that while winter cooling signals propagate efficiently into the entrance chamber, warm-season surface heating does not translate into proportional warming of the cave air. This pattern reflects the seasonally asymmetric nature of ventilation, which is also expressed in the monthly skewness characteristics: advective heat transfer is effective during episodic winter cold-air inflow, producing negatively skewed temperature distributions, whereas warm-season surface heating does not translate into proportional warming of the cave air when density contrasts no longer favor circulation.

The attenuation is further pronounced at SG-4, where correlation with SG-1 decreases to moderate values (r ≈ 0.68). The regression slope is shallow, and the scatter exhibits a broad spread, indicating that the surface signal reaches this depth only episodically. This behavior is consistent with the seasonal statistics showing increased variability during winter and strongly reduced variability during the warm season. The correlation therefore reflects a selective coupling, activated primarily under cold-season density-driven airflow and largely absent during thermally stratified conditions. In contrast, SG-5 shows only a very weak relationship with surface temperature (r ≈ 0.19; R^2 ≈ 0.03). This again confirms that SG-5 is mostly decoupled from advective heat transport and is controlled instead by conductive heat exchange with the surrounding rock mass.

Table 2 summarizes monthly correlation and regression parameters describing the relationship between surface air temperature (SG-1) and air temperature at the deepest monitored cave point (SG-4). The table integrates three complementary descriptors: the Pearson correlation coefficient (r), the regression slope (a), and the intercept (b), together with the coefficient of determination (R^2). Each parameter captures a different physical aspect of surface-cave coupling and ventilation dynamics. Based on its pronounced winter variability and strongest response to density-driven ventilation identified in the preceding analysis, SG-4 is used as the representative deep-cave reference location in the regression analysis.

The correlation coefficient (r) quantifies the strength of linear co-variation between surface and cave temperatures and thus provides a direct measure of how effectively surface thermal signals are transmitted to the cave interior. High r values during winter months (r ≈ 0.55-0.80) indicate response of SG-4 to external cooling, consistent with active density-driven ventilation. In contrast, near-zero or negative r values during summer and early autumn reflect the breakdown of this coupling under thermally stratified conditions, when advective exchange with external air is minimal. The regression slope (a) represents the sensitivity of SG-4 temperature to changes at the surface, expressed as the magnitude of cave temperature response per unit change in surface temperature. High slopes during winter months (e.g., a = 0.13 in January 2023) indicate that surface cooling produces a pronounced and proportional cooling response, confirming efficient advective heat transport by ventilated airflow. Conversely, slopes approaching zero during summer (e.g., a ≈ 0.000-0.003) demonstrate that changes in surface temperature have virtually no effect on SG-4, evidencing thermal decoupling and the dominance of stratified, non-advective conditions in cold-air trap environment.

Table 2. Monthly correlation and regression parameters between surface air temperature (SG-1) and air temperature at the deepest location of the cave (SG-4).

Period	r (Pearson)	a (slope)	b (intercept)	R²	Ventilation regime
Dec 2022	0.557	0.0565	4.6436	0.31	winter ventilation
Jan 2023	0.797	0.1324	4.3762	0.64	winter ventilation
Feb 2023	0.650	0.0794	3.1142	0.42	winter ventilation
Mar 2023	0.567	0.0377	3.8800	0.32	transitional
Apr 2023	0.638	0.0395	4.2560	0.41	transitional
May 2023	0.379	0.0135	5.0294	0.14	transition ➔ stable
Jun 2023	0.362	0.0062	5.4310	0.13	weak coupling
Jul 2023	0.017	0.00023	5.7622	0.0003	summer stratification
Aug 2023	0.245	0.00274	5.9192	0.060	summer stratification
Sep 2023	−0.215	−0.00224	6.1608	0.046	inverted gradient
Oct 2023	−0.036	−0.00025	6.2477	0.0013	inverted gradient
Nov 2023	0.652	0.0578	5.6613	0.43	ventilation onset
Dec 2023	0.732	0.0573	4.7634	0.54	winter ventilation
Jan 2024	0.636	0.1043	3.9327	0.40	winter ventilation
Feb 2024	0.296	0.0338	4.3639	0.09	weakened ventilation

Seasonal shifts in intercept values (b) reflect changes in the internal thermal reference state rather than direct surface forcing. Lower intercepts during winter correspond to the penetration of cold air into the lower cave sections, whereas higher intercepts during summer reflect the persistence of a stable, internally controlled temperature regime governed by heat exchange with the surrounding rock mass. The coefficient of determination (R^2) integrates the information contained in r and a by expressing how much of the variance in SG-4 temperature is statistically explained by surface temperature variability. High R^2 values during winter (up to 0.64 in January 2023) confirm that surface forcing dominates deep-cave temperature variability during active ventilation. In contrast, extremely low R^2 values in summer indicate that SG-4 temperature variability is almost entirely independent of surface conditions.

The combined use of correlation and regression parameters allows a process-based interpretation that goes beyond simple co-variation. Correlation identifies when coupling exists, the slope quantifies its intensity and the intercept reflects the evolving internal thermal reference of the cave. The seasonal progression of these parameters defines three distinct regimes: (i) a winter ventilation regime characterized by strong coupling and high sensitivity, (ii) transitional regimes with weakening or inverted relationships, and (iii) a summer stratified regime in which the cave interior is thermally isolated from the surface.

5. CONDITIONS FOR DENSITY DRIVEN EXCHANGE FLOW

Differences in air density have been recognized as the primary driver of exchange flow between the surface and underground environments, with cave air during cold periods being controlled predominantly by advective processes (Badino, 2010). This framework was later expanded through analytical models describing temperature distribution, entropy production, and the conditions required for the establishment of temperature driven air circulation, demonstrating that the magnitude and sign of the temperature difference between the cave and the atmosphere determine both the direction and intensity of airflow, while a critical density contrast governs the transition from weak to strong ventilation regimes (Badino, 2018). Studies of karst systems further show that cave temperature structure reflects the interaction between ventilation, hydrological conditions, and cave geometry; during winter, systems with permeable openings and relatively simple morphologies develop well-defined advective profiles, with turbulence becoming increasingly important under large density contrasts (Luetscher & Jeannin, 2004). More recent syntheses emphasize that the duration and intensity of ventilation episodes depend on the configuration of entrance and outlet openings, internal connectivity, and the amplitude of external temperature oscillations (Gabrovšek, 2023). Within this theoretical context, Samograd Cave provides an ideal natural setting for testing how observed microclimatic data conform to predicted ventilation patterns. Comparison of two consecutive winters allows assessment of how variations in external conditions, longitudinal temperature distribution, and internal cave geometry modulate the duration of ventilation episodes, their operational regime (T SG-1 < T SG-4 or T SG-1 > T SG-4), and the resulting microclimatic response of the cave. The analysis focuses on periods of intensive exchange flow during winter 2022/2023 and winter 2023/2024. Hourly air-temperature data were analyzed and grouped according to the thermal relationship between the surface (SG-1) and the deepest monitored location (SG-4). The choice of SG-4 as the representative deep cave site follows from the preceding analysis of its sensitivity to winter ventilation. Particular attention was given to episodes when surface air temperature falls below that of the cave interior temperature, and cold air intrusion into the cave triggers exchange flow. Although negative temperature differences occasionally persist into March, early April, and November, these episodes are short-lived and do not reach durations sufficient to establish sustained circulation; they are therefore not considered as part of the cold-period ventilation regime.

5.1. INTERPRETATION OF EPISODES LONGER THAN 100 HOURS DURING WINTER 2022/2023

Analysis of the winter period December 2022-February 2023 identified a total of 34 temporal episodes during which air temperature at SG-1 was lower than at SG-4, indicating conditions favorable for cold air intrusion (Figure 7). During analysis, these events were coded as 1, while periods with the opposite temperature relationship were coded as 0. The cumulative duration of episodes 1 amounted to 1346 hours, representing 62 % of the winter period. This proportion reflects the dominance of ventilated conditions during the season, although the overall frequency of sufficiently cold surface conditions was lower than expected under colder climatic regimes. For more detailed analysis, six episodes lasting more than

100 hours were selected (Table 3), as such long-duration events are expected to exert the strongest influence on cave conditions by introducing large volumes of cold air and maintaining a persistent thermal gradient that drives airflow. Although the number of selected episodes is limited, these episodes encompass both ventilated and non-ventilated states and therefore provide a representative basis for interpretation.

The selected episodes reveal a clear distinction between periods of active ventilation and periods without ventilation. Episodes 1, 2, 5, and 6 (Table 3) are characterized by a pronounced negative temperature gradient. Under these conditions, cold external air penetrates into the cave, and sustains ventilation over extended periods. In contrast, episodes 3 and 4 exhibit a reversed temperature relationship, with surface air temperature exceeding cave temperature. This thermal configuration inhibits downward airflow and results in a quiescent cave state without active ventilation. Ventilation episodes lasted between 104 and 307 hours and developed under persistently cold external conditions. Mean surface temperatures during these episodes were below 0 °C, with minimum values dropping below -7 °C and reaching almost -10 °C. Despite substantial variability in surface temperature, the cave interior remained remarkably stable, with SG-4 temperatures confined to a narrow range around 4-5 °C. The longest ventilation episode (ep. 5, 307 hours) coincides with both a very low mean surface temperature and the most pronounced negative ΔT mean, demonstrating that intense and sustained surface cooling prolongs ventilation duration by maintaining a strong and persistent thermal gradient.

Episodes without ventilation persisted for similarly long durations (161–172 hours) but occurred under fundamentally different thermal conditions. During these intervals, surface air temperatures remained consistently higher than cave air temperature, exceeding SG-4 by more than 3 °C on average, thereby suppressing density-driven inflow. Cave temperatures remained stable and comparable to those observed during ventilation episodes, indicating that changes in ventilation state are controlled primarily by surface conditions rather than by internal cave temperature. The resulting positive temperature differences eliminated the driving force for airflow, allowing a non-ventilated state dominated by slow conductive heat exchange with the surrounding rock mass to persist for extended periods.

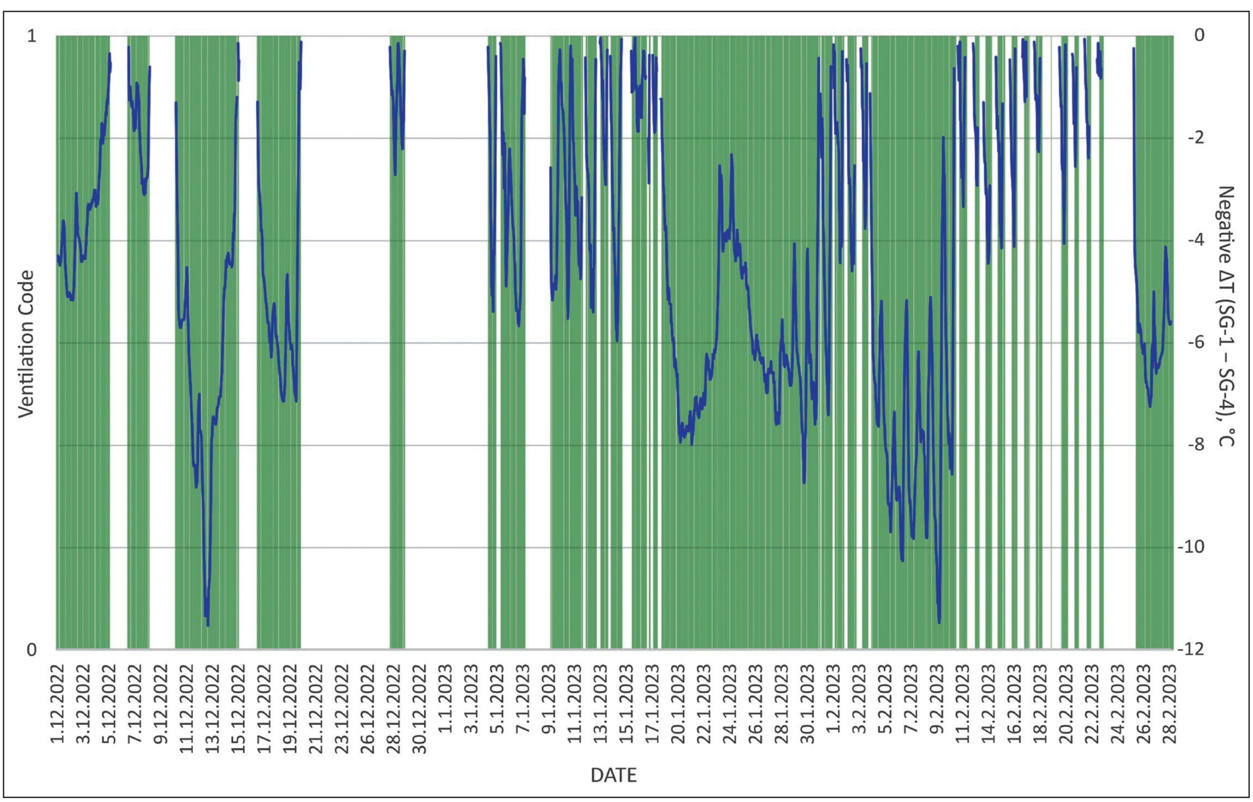

Figure 7. Winter ventilation episodes in Samograd Cave, 2022/2023 season. Binary ventilation code based on the temperature relationship between location SG-1 and SG-4, where 1 indicates periods with air T SG-1 < air T SG-4 (green) and 0 indicates periods with air T SG-1 > air T SG-4. Negative temperature differences ΔT (SG-1 – SG-4), showing the magnitude and temporal persistence of surface-cave thermal gradients during ventilated periods. Only negative ΔT values (blue) are shown in order to emphasize periods of active ventilation; positive ΔT values are discussed in the text and summarized in Table 3.

Analysis of temperature variability further highlights the contrasting behavior of surface and cave. At SG-1, both ventilated and non-ventilated episodes exhibit wide temperature ranges, reflecting strong meteorological variability. However, only episodes that include sufficiently low absolute surface temperatures develop negative thermal gradients capable of initiating ventilation. In contrast, SG-4 remains highly stable throughout all episodes, with minimal SD, underscoring the thermal buffering of the cave interior. Across all selected episodes, the mean ΔT provides the clearest indicator of ventilation state. These results confirm that winter ventilation is governed primarily by the magnitude and persistence of the thermal contrast between the surface and the cave interior, while the cave itself remains thermally stable and acts as a passive boundary condition in the ventilation system.

5.2. INTERPRETATION OF EPISODES LONGER THAN 100 HOURS DURING WINTER 2023/2024

Analysis of the winter period 2023/2024 identified a total of 47 temporal episodes during which air temperature at SG-1 was lower than at SG-4 (Figure 8). The cumulative duration of episodes coded as 1 amounted to 1002 hours, representing 46 % of the winter period. Compared to the previous season, this lower proportion reflects a higher frequency of interruptions by warmer surface conditions, despite the presence of several long-lasting cold phases.

For more detailed analysis, five episodes with durations exceeding 100 hours were selected (Table 4), based on the same assumption applied in the previous section. Although the number of selected episodes is small (n = 5), several consistent patterns can be identified.

Selected ventilation episodes (code 1) lasted between 122 and 184 hours. All three ventilation episodes share several common features. Mean surface air temperatures at SG-1 were below 0 °C (−0.33, −3.68, and −2.04 °C), while SG-4 temperatures were ranging between 3.47 and 4.71 °C. The resulting mean temperature differences were strongly negative (ΔT mean between -5.04 and -7.47 °C), indicating persistent and effective thermal forcing for downward airflow. The longest ventilation episodes (1 and 3, both 184 h) coincide with the most pronounced negative gradients, particularly episode 3, which exhibits the lowest mean surface temperature (-3.68 °C) and the most extreme ΔT mean (−7.47 °C). Episodes without ventilation lasted 103 and 162 hours and developed

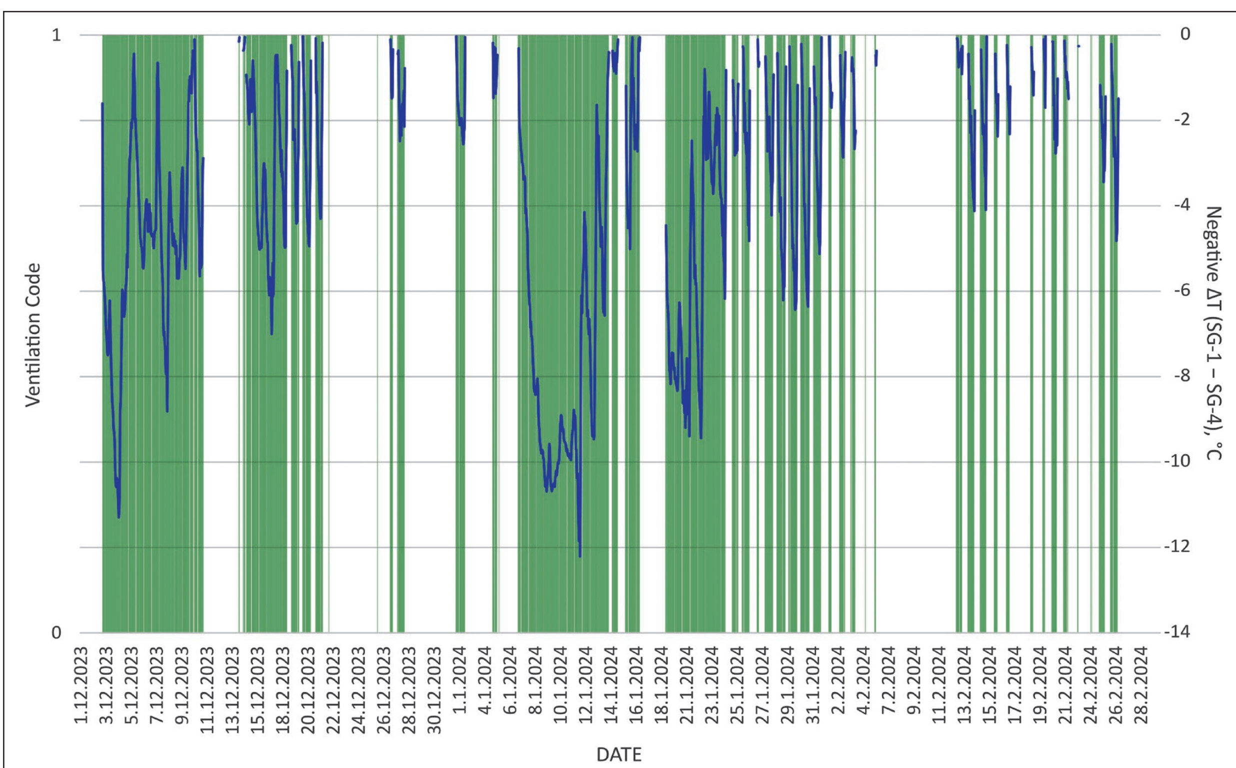

Figure 8. Winter ventilation episodes in Samograd Cave, 2023/2024 season. Binary ventilation code is based on the temperature relationship between location SG-1 and SG-4, where 1 indicates periods with air T SG-1 < air T SG-4 (green) and 0 indicates periods with air T SG-1 > air T SG-4. Negative temperature differences ΔT (SG-1 – SG-4), showing the magnitude and temporal persistence of surface-cave thermal gradients during ventilated periods. Only negative ΔT values (blue) are shown in order to emphasize periods of active ventilation; positive ΔT values are discussed in the text and summarized in Table 4.

*Table 3. Selected episodes with air circulation or stagnant conditions longer than 100 h during Winter 2022/2023.**

Episode	Start	End	Code	Duration (h)	SG-1 min (°C)	SG-1 mean (°C)	SG-1 SD (°C)	SG-4 mean (°C)	SG-4 SD (°C)	ΔT mean (°C)	ΔT SD (°C)
1	01.12.2022 00:00	05.12.2022 07:00	1	104	-0.28	1.54	1.34	5.05	0.11	-3.52	1.23
2	10.12.2022 14:00	15.12.2022 12:00	1	119	-7.87	-2.18	2.57	4.09	0.62	-6.61	2.34
3	20.12.2022 17:00	27.12.2022 20:00	0	172	4.92	8.30	1.51	4.97	0.21	3.46	1.39
4	29.12.2022 02:00	04.01.2023 18:00	0	161	5.28	8.38	1.56	5.25	0.06	3.13	1.60
5	18.01.2023 18:00	31.01.2023 12:00	1	307	-5.64	-1.96	2.52	3.97	0.52	-5.93	1.51
6	04.02.2023 16:00	11.02.2023 11:00	1	164	-9.95	-5.13	2.76	2.41	0.56	-7.59	2.05

**The table includes only parameters directly used in the interpretation of long-duration ventilation episodes. For SG-1 (surface), minimum temperature, mean, and standard deviation (SD) are reported to characterize the intensity and variability of external forcing. For SG-4 (cave), mean temperature and SD are retained to document thermal stability of the cave interior. The mean temperature difference (ΔT = SG-1 – SG-4) and its SD quantify both the direction and strength of the thermal gradient driving (or inhibiting) convective ventilation. Code 1 = active ventilation; 0 = no ventilation.*

under thermal conditions opposite to those observed during ventilation episodes. In both cases, mean surface temperatures were higher (7.98 and 7.91 °C at SG-1), exceeding cave air temperature (SG-4) by more than 2.5 °C and thereby eliminating the density-driven forcing required for downward airflow. Cave temperatures remained stable at approximately 4.5-5.4 °C, and the resulting positive ΔT mean values (2.57 and 3.42 °C) eliminated the driving force required for convective airflow.

Analysis of temperature variability further highlights the contrasting behavior of surface and cave environments. At SG-1, standard deviations during ventilation episodes are relatively high (2.51-3.30 °C), reflecting strong meteorological variability and intermittent cold extremes critical for maintaining negative thermal gradients. In contrast, SG-4 remains more stable throughout all episodes, with standard deviations consistently below 0.9 °C. As in the previous winter, the mean temperature difference ΔT mean provides a robust indicator of ventilation state: values between -5.0 and –7.5 °C correspond to active ventilation, while positive values around +3 °C are associated with stagnation.

The comparison of the two consecutive winters confirms that winter ventilation in Samograd Cave is controlled primarily by the magnitude and persistence of the surface-cave thermal gradient, rather than by the frequency of cold events alone. Although the Winter of 2023/2024 featured fewer long-duration episodes than 2022/2023, several episodes were longer and thermally more extreme, characterized by stronger and more sustained negative ΔT values. In both winters, prolonged ventilation occurred exclusively under persistently negative surface-cave temperature differences, with the duration and intensity of ventilation reflecting both the magnitude and temporal persistence of the thermal gradient. Despite interannual differences in ventilation intensity and the magnitude of negative ΔT values, cave air temperature at SG-4 remained quite stable as a result of the strong buffering effect of the surrounding rock mass.

6. CO_2 AS AN INDICATOR OF VENTILATION PROCESSES AND MICROCLIMATIC DYNAMICS IN SAMOGRAD CAVE

6.1. ANALYTICAL FRAMEWORK

Under appropriate conditions in caves, CO_2 accumulates during periods of weak or absent ventilation as a result of chemical and biological processes, including anthropogenic contributions, whereas during winter periods temperature-driven inflow of cold air efficiently flushes the cave atmosphere, leading to a decrease in CO_2 concentration (Covington, 2015; Lang et al., 2017; Kukuljan et al., 2021; Buzjak et al., 2024). In caves with effective winter ventilation, CO_2 concentrations may approach atmospheric background values. CO_2 therefore represents an integrated response to the balance between internal sources and ventilation efficiency and can be used as an indicator of cave air exchange, particularly when interpreted together with temperature-derived ventilation proxies. The aim of this analysis is to assess to what extent CO_2 concentrations can serve as an indicator of the ventilation regime of Samograd Cave and how they relate to temperature gradients between the surface and the cave interior.

The analytical approach applied here treats cave ventilation as a process controlled primarily by density-driven contrasts between the surface and the cave expressed as temperature difference (ΔT). All ΔT indicators were defined relative to SG-4, which represents the deepest cave location where the direct influence of temperature-driven ventilation is still clearly expressed. Using a single reference point ensures that both the sign and magnitude of ΔT retain the same physical meaning across all indicators throughout the annual cycle.

The following temperature differences were defined:

ΔT_{14} = T(SG-1) - T(SG-4)

ΔT_{24} = T(SG-2) - T(SG-4)

ΔT_{34} = T(SG-3) - T(SG-4)

The indicators ΔT_{14}, ΔT_{24}, and ΔT_{34} describe surface-to-cave thermal forcing and thus the potential for ventilation driven by temperature contrasts.

Correlations between ΔT indicators and CO_2 concentrations measured at different cave locations are interpreted within this framework. ΔT represents the common driving signal describing the ventilation state of the cave, while CO_2 concentrations here represent spatially differentiated system responses to that state. The resulting relationships therefore do not imply direct point-to-point coupling between specific temperature and CO_2 measurement sites, but quantify how CO_2 concentrations at different locations respond to the same ventilation forcing. In addition to correlation-based analysis, monthly spot measurements of CO_2 concentrations are used to describe the seasonal evolution of cave air composition and to compare CO_2 dynamics with monthly mean air temperatures. Although monthly CO_2 measurements represent a coarse temporal sampling, they provide a robust integrated signal of the prevailing ventilation regime.

6.2. CO_2 RESPONSE TO DENSITY-DRIVEN VENTILATION

Monthly CO_2 concentrations show a pronounced seasonal cycle at all monitoring locations (Figure 9). At surface sites SG-1 and SG-2, CO_2 concentrations remain close to atmospheric values throughout the year (approximately 400-450 ppm), with only minor seasonal variability. In contrast, interior sites SG-3, SG-4, and SG-5 exhibit a strong bimodal pattern. During winter and early spring, CO_2 concentrations remain low and relatively stable (approximately 410-520 ppm), indicating efficient ventilation and air exchange with the external atmosphere. From late spring onward, CO_2 concentrations increase rapidly, reaching maxima during summer and early autumn, with peak values exceeding 2200 ppm. This seasonal accumulation reflects prolonged stagnation and thermal isolation of the cave atmosphere during warm periods.

CO_2 concentrations are consistently higher at SG-5 than at SG-4 throughout most of the year, despite SG-5 being located higher within the cave (Figure 9B). This counter-intuitive vertical pattern reflects the persistent thermal stratification of cave air. During winter ventilation, colder and denser external air accumulates preferentially in the lower part of the passage (SG-4), where it efficiently flushes CO_2. In contrast, the air at SG-5 remains warmer and less dense, forming an upper stratified layer less influenced by the ventilation. Under such conditions, downward mixing of CO_2 is strongly limited, and the vertical density structure effectively inhibits homogenization of the cave atmosphere. As a result, CO_2 concentrations remain higher in the upper part of the passage (SG-5) than at the lower site (SG-4), even during periods of active winter ventilation. During warm periods, the upper zone (SG-5) becomes more strongly coupled to epikarst CO_2 sources, while the near-complete suppression of density-driven ventilation limits effective air exchange with the exterior, resulting in systematically higher CO_2 concentrations (Buzjak et al., 2024). This pattern demonstrates that thermal stratification, controlled by temperature-driven density contrasts, exerts a first-order control on the vertical distribution of CO_2 within the cave. It also highlights the importance of cave geometry and stratification in controlling CO_2 distribution, beyond simple elevation effects.

Comparison with monthly mean air temperatures (Figure 9A) shows that low CO_2 concentrations coincide with periods when surface air temperatures are lower than cave interior temperatures, whereas CO_2 accumulation occurs when surface temperatures exceed those of the cave. Monthly CO_2 concentrations therefore provide an integrated seasonal signal that mirrors the temperature-controlled ventilation regime inferred from continuous air-temperature measurements.

Pearson correlation coefficients between monthly CO_2 concentrations and temperature-derived ventilation proxies are summarized in Table 5. The table focuses on

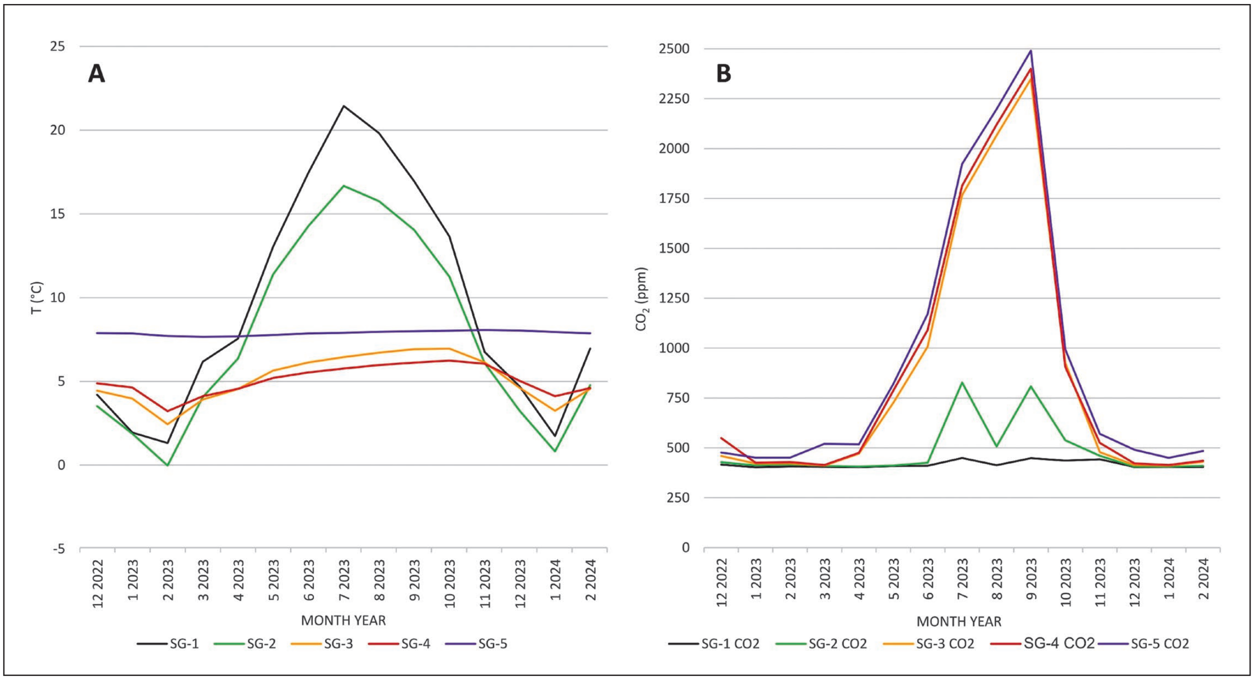

Figure 9. Dynamics of air temperature and CO_2 concentration in Samograd Cave. A - Monthly mean air temperature at monitoring sites FROM SG-1 to SG-5. B - Monthly spot CO_2 concentrations measured at the same sites. SG-2 remains close to atmospheric values, whereas interior sites (SG-3 to SG-5) show pronounced warm-season accumulation and winter minima consistent with efficient ventilation.

interior and entrance-proximal locations (SG-2 to SG-4), which are directly relevant to cave ventilation processes.

The surface-interior temperature difference ΔT_{14} shows a clear positive relationship with CO_2 concentrations at all locations, with correlation strength increasing from the entrance towards the cave interior. Moderate correlations at SG-2 and strong correlations at SG-3 and SG-4 indicate that increasing surface-cave thermal contrast is systematically associated with enhanced CO_2 flushing throughout the cave. The strong correlation between CO_2 concentrations at SG-5 and the surface-cave temperature difference ΔT_{14} ($r = 0.862$) does not imply direct advective inflow reaching this upper part of the passage. Instead, ΔT_{14} acts as a proxy of the overall ventilation state of the cave system. During winter, when ΔT_{14} is negative and the cave is ventilated, CO_2 concentrations decrease throughout the cave, including at SG-5,

Table 5. Pearson correlation coefficients (r) between monthly CO_2 concentrations at each location and three temperature-difference indicators (ΔT) used as proxies of ventilation forcing and internal redistribution.

Location	r (ΔT_{14})	r (ΔT_{24})	r (ΔT_{34})
SG-2	0.673	0.657	0.619
SG-3	0.846	0.837	0.772
SG-4	0.851	0.844	0.775
SG-5	0.862	0.853	0.787

as a result of system-wide flushing, reduced CO_2 input from epikarst and soil sources, and the resetting of background cave-air composition to low values. In contrast, during warm periods with positive ΔT_{14}, ventilation is suppressed and CO_2 accumulates at all locations, including SG-5, due to limited air exchange and enhanced internal sources. The high correlation therefore reflects a coherent, regime-scale response of CO_2 at SG-5 to seasonal ventilation states, rather than local airflow conditions.

A very similar response pattern is observed for ΔT_{24}, confirming that temperature gradients acting near the cave entrance exert a strong control on cave-wide ventilation efficiency and CO_2 dynamics. Correlations between CO_2 concentrations and ΔT_{34} remain positive but are consistently lower than those obtained for ΔT_{14} and ΔT_{24}. This reduction reflects the diminishing influence of direct surface forcing and the increasing role of internal cave geometry and air redistribution processes.

To further evaluate the temporal conditions under which air density-driven ventilation becomes effective, hourly air temperature data at SG-1 and SG-4 were combined with an hourly CO_2 record at SG-4 (Figure 10). The temporal evolution of ΔT_{14} and CO_2 concentration at SG-4 shows that sustained periods of negative ΔT_{14} during the winter are consistently associated with a pronounced and long-lasting decrease in CO_2 concentration. These intervals reflect prolonged cold-air inflow

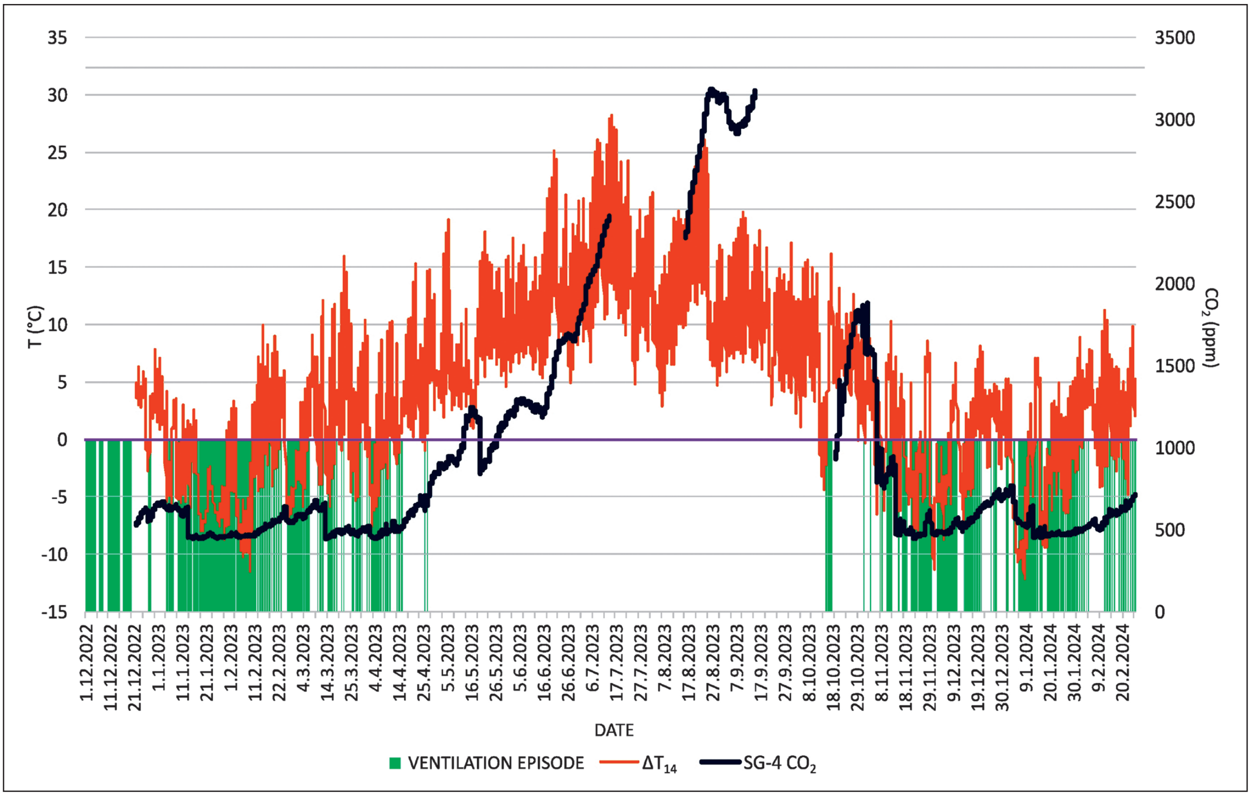

Figure 10. Hourly time series of the surface-cave temperature difference ΔT_{14} and CO_2 concentration at SG-4. Green bars indicate periods when $\Delta T_{14} < 0$, i.e., when surface air is colder than cave air and density-driven inflow is possible. Sustained periods of negative ΔT_{14} during winter are associated with density-driven ventilation and a pronounced, persistent decrease in CO_2 concentration at SG-4, reflecting effective flushing of cave air. In contrast, short-lived negative ΔT_{14} episodes outside the winter period do not produce a comparable CO_2 response. The horizontal purple line marks $\Delta T_{14} = 0$ °C.

and effective ventilation of the cave atmosphere. In contrast, negative ΔT_{14} episodes occurring during transitional seasons are typically short-lived and highly variable. Although such episodes may temporarily indicate conditions favorable for ventilation, they do not result in a comparable or sustained reduction in CO_2 concentration. These observations suggest that sustained negative temperature gradients are necessary for pronounced CO_2 reduction, whereas short-lived episodes appear insufficient to produce a comparable response.

Overall, the combined behavior of CO_2 concentrations and temperature-derived ventilation proxies demonstrates that monthly CO_2 measurements, despite their coarse temporal resolution, provide an exceptionally reliable integrated indicator of the seasonal ventilation regime of Samograd Cave. The strong and systematic relationships confirm that temperature gradients (and resulting differences in air density) are the primary driver of seasonal ventilation and that CO_2 dynamics quantitatively capture the transition between winter ventilation and summer microclimatic isolation, independently corroborating the processes inferred from air temperature analysis.

7. CONCLUSION

Understanding cave ventilation requires more than documenting seasonal variability - it requires identifying the physical conditions under which air exchange is initiated, sustained, or suppressed. By combining continuous air-temperature and CO_2 monitoring in Samograd Cave (Croatia) with limited but functionally effective atmospheric exchange with the surface, this study provides a physically explicit interpretation of how and when airflow governs cave microclimate behavior.

The analysis of Samograd Cave shows that its microclimate is organized around two distinct and internally consistent states controlled by density-driven air exchange with the surface. Continuous air-temperature measurements demonstrate that the cave airflow alternates between a winter regime characterized by active convective ventilation and a summer regime dominated by stagnation, cold-air trapping and vertical temperature stratification. This bimodality is not a descriptive classification, but a measurable system response expressed through the sign, magnitude, and persistence of surface-cave temperature gradients. Air-temperature data from data loggers measured in hourly temporal resolution reveal that the cave-surface relationship is strongly asymmetric in time and controlled by the direction of the surface-cave temperature gradient. Statistical analyses show that coherent cave cooling occurs only when surface air becomes colder and denser than cave air (winter), resulting in inflow of air from the surface into the cave. Under these conditions, temperature changes propagate progressively from the entrance toward the interior, indicating the development of exchange airflow. In contrast, when surface temperatures exceed cave temperatures (warm periods), positive gradients suppress air exchange, the cave becomes thermally decoupled from the surface, and ventilation effectively ceases. The cave acts as a cold air trap with evident vertical air temperature stratification. These results demonstrate that cave ventilation is governed by a threshold-controlled, temperature-driven density contrast. The comparison of consecutive winters further refines this interpretation by demonstrating that ventilation intensity is governed primarily by the cumulative effect of thermal forcing. Fewer cold episodes may result in stronger ventilation when thermal gradients persist over longer periods, while frequent but short-lived cold events produce weaker overall ventilation. This finding resolves an apparent paradox in cave ventilation studies and underscores persistence, rather than event frequency, as the dominant control on winter airflow circulation.

CO_2 concentration measurements independently corroborate the temperature-based interpretation of ventilation regimes. Periods of active winter ventilation are consistently associated with declining CO_2 concentrations, indicating efficient flushing of the cave atmosphere, whereas prolonged summer stagnation leads to CO_2 accumulation. The close correspondence between density-defined airflow states and CO_2 dynamics confirms CO_2 as an integrative indicator of ventilation efficiency, capable of validating physical interpretations derived from thermal data alone.

Taken together, these results define Samograd Cave as a seasonally activated density-driven exchange flow system with two microclimatic modes. Beyond site-specific observations, this study provides a physically grounded framework for interpreting cave ventilation as a threshold-controlled process governed by the sign, magnitude, and persistence of surface-cave thermal gradients. This framework is directly transferable to caves with similar morphology and provides a robust basis for interpreting cave climate dynamics, assessing ecological and biogeochemical processes, and evaluating sensitivity to anthropogenic pressures such as tourism. More broadly, the study demonstrates that carefully analyzed temperature data, when combined with CO_2 as a process indicator, are sufficient to resolve the dominant ventilation mechanisms that characterize cave microclimates.

ACKNOWLEDGEMENTS

This work has been supported by Croatian Science Foundation under the project "Dynamics and distribution of CO_2 in karst vadose and epiphreatic zone (CARDIKARST) (IPS-2022-02-2260)".

We thank to Cave Park Grabovača (Perušić, Croatia) for logistics; our deepest thanks go to Jelena Milković, Marko Danilović, and Mario Paral. We extend our gratitude to Suzana Buzjak, Ivana Živković, Iztok Miklavčič, and Caving Club Samobor for their occasional support in fieldwork, as well as Helena Varga, and Filip Patčev for their assistance with data organization and field work.

REFERENCES

AZ Instrument Corp., n.d. AZ CO2 Meter 77535. https://www.az-instrument.com.tw/en/product-616381/RH-Temp-CO2-Meter-77535-AZ-EB.html [Accessed 15. January 2026.]

Badino, G., 2010. Underground meteorology – what's the weather underground? Acta Carsologica, 39(3): 427–448. https://doi.org/10.3986/ac.v39i3.74

Badino, G., 2018. Models of temperature, entropy production and convective airflow in caves. In: Parise, M., Gabrovšek, F., Kaufmann, G., Ravbar, N. (Eds.), Advances in Karst Research: Theory, Fieldwork and Applications. Geological Society, London, Special Publications, 466: 359–379. https://doi.org/10.1144/SP466.24

Buzjak, N., Bočić, N., Pahernik, M., 2020. Geomorphological heritage of the Significant landscape Risovac-Grabovača. Acta Geographica Croatica, 45/46: 49-67. https://doi.org/10.21861/AGC.2019.45-46.04

Buzjak, N., Gabrovšek, F., Perşoiu, A., Pennos, C., Paar, D. & Bočić, N., 2024. CO_2 Emission from Caves by Temperature-Driven Air Circulation - Insights from Samograd Cave, Croatia, Climate, 12(12): 199. https://doi.org/10.3390/cli12120199

CO2Meter, 2016. CO2Meter data logger CM-0018. https://co2meters.com/Documentation/Manuals/Manual-CM-0016-Data-Logger.pdf [Accessed 15. January 2026.]

Covington, M.D., 2015. The importance of advection for CO_2 dynamics in the karst critical zone: An approach from dimensional analysis. In Feinberg, J., Gao, Y., and Alexander, E.C., Jr. (Eds.), Caves and Karst Across Time: Geological Society of America Special Paper 516, https://doi.org/10.1130/2015.2516(09)

de Freitas, C.R., 1987. Cave climate: assessment of heat and moisture exchange. Journal of Climatology, 7: 553–569. https://doi.org/10.1002/joc.3370070604

Drogue, C., 1985. Geothermal gradients and ground water circulation in fissured and karstic rocks: The role played by the structure of the permeable network. Journal of Geodynamics, 4: 219–231. https://doi.org/10.1016/0264-3707(85)90061-4

Filipčić, A., 1998. Klimatska regionalizacija Hrvatske po W. Köppenu za standardno razdoblje 1961. – 1990. u odnosu na razdoblje 1931. – 1960. [Climatic regionalization of Croatia according to W. Köppen for the standard period 1961-1990 compared to the period 1931-1960.]. Acta Geographica Croatica, 33(1): 7-14.

Gabrovšek, F., 2023. How do caves breathe: The airflow patterns in karst underground. PLOS ONE, 18(4), e0283767, https://doi.org/10.1371/journal.pone.0283767

Gil, D., Sánchez-Gómez, M., Tovar-Pescador, J., 2025. Microclimate Variability in a Highly Dynamic Karstic System. Geosciences, 15(8): 280. https://doi.org/10.3390/geosciences15080280

Kukuljan, L., Gabrovšek, F., Covington, M.D., Johnston, V.E. 2021. CO_2 dynamics and heterogeneity in a cave atmosphere: role of ventilation patterns and airflow pathways. Theoretical and Applied Climatology, 146 (1): 91–109. https://doi.org/10.1007/s00704-021-03722-w.

Lang, M., Faimon, J., Godissart, J., Ek, C. 2017. Carbon dioxide seasonality in dynamically ventilated caves: the role of advective fluxes. Theoretical and Applied Climatology, 129: 1355–1372. https://doi.org/10.1007/s00704-016-1858-y

Luetscher, M. & Jeannin, P.-Y., 2004. Temperature distribution in karst systems: the role of air and water fluxes. Terra Nova, 16(6): 344–350. https://doi.org/10.1111/j.1365-3121.2004.00572.x

ONSET Hobo, n.d. HOBO U23 Pro v2 Temperature/Relative Humidity Data Logger. https://www.onsetcomp.com/products/data-loggers/u23-001a [Accessed 15. January 2026.]

Persoiu, A., Buzjak, N., Onaca, A., Pennos, C., Sotiriadis, Y., Ionita, M., Zachariadis, S., Styllas, M., Kosutnik, J., Hegyi, A., Butorac, V. 2021. Record summer rains in 2019 led to massive loss of surface and cave ice in SE Europe. The Cryosphere, 15(5): 2383–2399. https://doi.org/10.5194/tc-15-2383-2021

Pulina, M., 1968. Термика воздуха в пещерах польских Татр [Air temperature regime in the caves of the Polish Tatras], Proceedings of the 4th International Congress of Speleology in Yugoslavia, Vol. III. Ljubljana: Speleological Society of Yugoslavia, 195–204.